Catalyst Development for Isobutanol Synthesis

Marcelo J. L. Gines, Mingting Xu, Anne-Mette Hilmen, and <u>Enrique Iglesia</u>
Department of Chemical Engineering, University of California, Berkeley, CA 94720-1462

Introduction

Isobutanol is a potential fuel additive or precursor to methyl tert-butyl ether (MTBE). Alkali-promoted $Cu/ZnO/Al_2O_3$ and $Cu/MgO/CeO_2$ materials catalyze the formation of isobutanol from CO and H_2 at temperatures (573-623 K) that allow their use in slurry reactors.[1-3] These catalysts were prepared by coprecipitation and incipient wetness methods. The number of Cu surface atoms was measured by N_2O titration. A new $^{13}CO_2/^{12}CO_2$ isotopic switch method was developed to probe directly the density of basic sites on solid basic catalysts at temperatures typical of base-catalytic reactors. This method measures the dynamics of adsorption-desorption processes at equilibrium and the density of sites that interact reversibly with CO_2 at rates comparable to turnover rates for useful catalytic reactions. The addition of K to MgO and $Cu_{0.5}Mg_5CeO_x$ increases the number of such kinetically available adsorption sites.

Isobutanol Synthesis from CO/H_2 Mixtures

Catalysts have been studied for the synthesis of alcohols from H_2/CO mixtures (4.5 MPa, 573-633K, $H_2/CO=1$) in a packed-bed reactor. The effects of space velocity on alcohol selectivities are shown in Figure 1 for Cs-$Cu/ZnO/Al_2O_3$ and K-$Cu_{0.5}Mg_5CeO_x$ catalysts. The CO conversion does not increase linearly with increasing bed residence time because the predominant methanol synthesis steps approach equilibrium. Isobutanol and higher alcohols form in secondary chain growth reactions and therefore their concentrations increase with increasing bed residence time. C_2-C_3 alcohols are intermediate products that undergo further chain growth and their selectivity therefore reaches a maximum value at intermediate residence times.
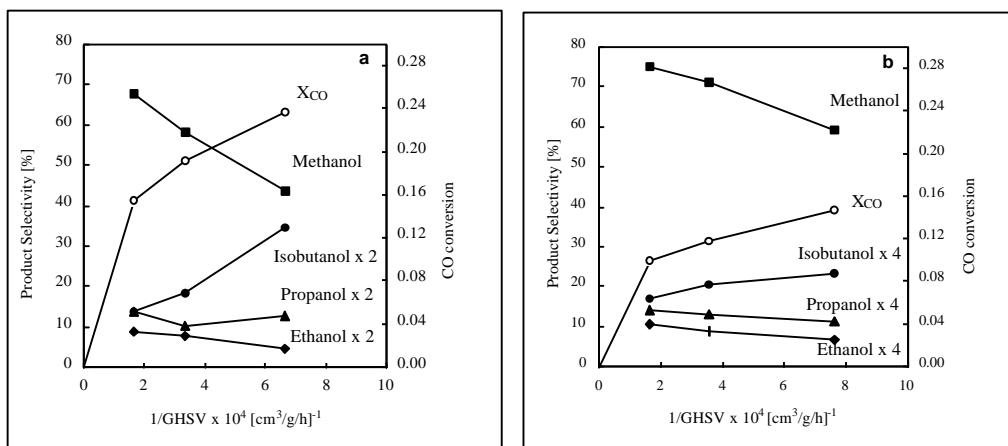
Figure 1. CO conversion and product selectivities vs. space velocity on: a) Cs-$Cu/ZnO/Al_2O_3$; b) K-$Cu_{0.5}Mg_5CeO_x$. [583 K, 4.5 MPa, $CO/H_2 = 1$, product selectivities are on CO_2-free basis.]

Isobutanol selectivity increases monotonically with increasing bed residence time for Cs-$Cu/ZnO/Al_2O_3$ because it is a kinetic end-product of aldol-type condensation processes. The increase in isobutanol selectivity is less marked on K-$Cu_{0.5}Mg_5CeO_x$, because chain growth reactions are inhibited by CO_2 (or H_2O) more strongly on K-$Cu_{0.5}Mg_5CeO_x$ than on Cs-$Cu/ZnO/Al_2O_3$. CO_2 (or H_2O) inhibit aldol-type coupling reactions during isobutanol synthesis on K-promoted $Cu_{0.5}Mg_5CeO_x$ catalysts. Weaker basic sites on Cs-$Cu/ZnO/Al_2O_3$ appear to be less sensitive to CO_2 poisoning and therefore isobutanol selectivities reach higher values than on K-$Cu_{0.5}Mg_5CeO_x$ as bed residence time and CO conversion increase.

Effect of Alcohol Addition on Isobutanol Synthesis

Table 1 shows the effects of ethanol and 1-propanol addition on product selectivities on 2.9 wt. % Cs-$Cu/ZnO/Al_2O_3$. The selectivity to 1-propanol increases when ethanol is added, as expected from its formation via C_1 addition to C_2 intermediates. 1-Propanol can be formed both by aldol coupling and by carbonylation pathways. The

selectivity to isobutanol also increases when ethanol is added. Isobutanol is formed only by C_1 addition to 1-propanol. 1-Butanol selectivity also increased; it is formed both by carbonylation and by ethanol aldol self-condensation pathways. Ethanol self-condensation can also lead to 2-propanol (after retro-aldol reactions) and 2-butanol. Increased selectivity for 2-propanol shows that self-condensation does occur, and that 1-butanol is predominantly formed by ethanol self-condensation and not by linear chain growth pathways.

Table 1. Ethanol and 1-propanol addition on 2.9 wt. % Cs-Cu/ZnO/Al$_2$O$_3$. [583 K, 4.5 MPa, 6000 cm^3/g-cat-h, H$_2$/CO/Ar/C$_2$H$_5$OH = 44.5/44.5/0.1/0.02, H$_2$/CO/Ar/C$_3$H$_7$OH = 44.5/44.5/0.1/0.01]

	None	Ethanol	None	Propanol	None
CO conversion [%]	15.4	14.8	14.8	14.2	14.3
Selectivities [% C; CO$_2$ free]					
Methanol	67.6	67.5	69.2	69.9	71.0
Ethanol	4.4	12.2	4.3	3.5	4.2
1-Propanol	6.9	21.6	7.2	24.3	7.0
2-Propanol	0.7	2.8	0.6	1.1	0.6
2-Methyl-1-propanol	6.9	14.8	6.3	28.6	5.9
1-Butanol	1.0	2.9	1.0	2.0	0.9

The large increase in isobutanol selectivity during 1-propanol addition confirms that isobutanol is formed predominantly by aldol-type C_1 addition to C_3 species derived from 1-propanol. The ratio of the increase in isobutanol selectivity to the increase in 1-butanol selectivity when propanol is added shows that aldol condensation pathways are about 22 times faster than linear chain growth on 2.9 wt. % Cs-Cu/ZnO/Al$_2$O$_3$ at the conditions of our study. The ratio of increase in isobutanol selectivity to increase in 1-butanol selectivity on a 1.2 wt. % K-Cu$_{7.5}$Mg$_5$CeO$_x$ catalyst when 1-propanol was added (not shown) was somewhat lower (~9) than for the 2.9 wt. % Cs-Cu/ZnO/Al$_2$O$_3$, but aldol-type C_1 addition is still the predominant chain growth pathway on K-Cu$_{7.5}$Mg$_5$CeO$_x$.

Table 2 shows product selectivities and isobutanol synthesis rates for 1.0 wt % K-Cu$_{0.5}$Mg$_5$CeO$_x$, 1.0 wt % K-Cu$_{0.5}$Mg$_5$ZnO$_x$, 1.0 wt % K-0.25 wt % Pd-Cu$_{0.5}$Mg$_5$CeO$_x$, 0.9 wt % K-Cu$_{7.5}$Mg$_5$CeO$_x$, 1.2 wt % Cs-Cu/ZnO/Al$_2$O$_3$, 2.9 wt % Cs-Cu/ZnO/Al$_2$O$_3$ at similar conversions. The 2.9 wt. % Cs-Cu/ZnO/Al$_2$O$_3$ catalyst showed the highest isobutanol synthesis rates at CO conversions of about 15%. The molar ratio of isobutanol to methanol is, however, only about 0.03. Decreasing the space velocity increased this ratio to 0.1 (at 1500 cm^3/g/h). K-Cu$_y$Mg$_5$CeO$_x$ catalysts show lower isobutanol synthesis rates than Cs-Cu/ZnO/Al$_2$O$_3$ as conversion increases because of stronger CO$_2$ inhibition effects, but reach very similar rates of isobutanol synthesis at low CO$_2$.

Table 2. Comparison of K-Cu$_y$Mg$_5$CeO$_x$ and Cs-Cu/ZnO/Al$_2$O$_3$ catalysts. [583 K, 4.5 MPa, H$_2$/CO=1]

Catalyst	1.0 wt % K-Cu$_{0.5}$Mg$_5$CeO$_x$	1.0 wt % K-Cu$_{0.5}$Mg$_5$ZnO$_x$	1.0 wt % K-0.25 wt % Pd-Cu$_{0.5}$Mg$_5$CeO$_x$	0.9 wt % K-Cu$_{7.5}$Mg$_5$CeO$_x$	1.2 wt % Cs-Cu/Zn/AlO$_x$	2.9 wt % Cs-Cu/Zn/AlO$_x$
CO conversion [%]	14.7	13.6	13.1	17.6	15.0	15.4
Isobutanol rate [g/kg/h]	3.7	12.2	6.9	9.5	8.1	20.3
Selectivities [%C; CO$_2$ free]						
Methanol	63.1	64.6	68.4	57.4	63.5	67.6
Ethanol	1.8	5.7	3.0	2.0	3.9	4.4
1-Propanol	3.0	6.4	4.1	3.1	2.3	6.9
2-Methyl-1-propanol	6.2	5.3	6.2	3.3	3.3	6.9
DME+hydrocarbons	11.5	4.0	9.9	20.6	12.5	3.3
i-BuOH/MeOH molar ratio	0.026	0.020	0.023	0.014	0.013	0.026

CO$_2$ inhibition effects also reflect an increase in the steady-state oxygen coverage on Cu crystallites with increasing CO$_2$ concentration. Cu sites are required both in methanol synthesis steps and in bifunctional (metal-base) chain growth

reactions of alcohols The surface of small Cu crystallites strongly interacting with CeO_x species has a higher oxygen affinity than larger Cu crystallites and are more strongly inhibited by CO_2. Increasing the Cu content in $K-Cu_yMg_5CeO_x$ leads to larger Cu crystallites, weaker inhibition effects, and higher isobutanol synthesis rates (Table 2). The addition of small amounts of Pd to $K-Cu_{0.5}Mg_5CeO_x$ almost doubles isobutanol synthesis rates (Table 2), because Pd species are less easily oxidized during higher alcohols synthesis and remain active for hydrogen adsorption-desorption steps required in bifunctional chain growth pathways at higher CO_2 concentrations. Similarly, the use of Mg_5ZnO_x high surface area supports leads to weaker CO_2 inhibition effects and to significantly higher isobutanol synthesis rates, even for catalysts with low Cu content (Table 2). The absence of CeO_x species avoids strong metal-support interactions that favor the oxidation of Cu metal surface during reaction. In addition, dimethylether and hydrocarbons selectivities decreased markedly when Mg_5CeO_x supports were replaced with Mg_5ZnO_x (Table 2).

Isotopic Tracer Studies of Alcohol Synthesis Pathways

Isotopic tracer studies of alcohol synthesis pathways were carried out on 1.0 wt % $K-Cu_{0.5}Mg_5CeO_x$ catalysts using a mixture of $^{13}CO/H_2$ and $^{12}CH_3OH$ in order to probe the roles of CO and methanol in chain growth pathways. At the conditions of our study (538 K, 2.0 MPa, and $H_2/^{13}CO = 1$) the equilibrium partial pressure of methanol is 86.6 kPa. The partial pressure of $^{12}CH_3OH$ in the feed was 13.3 kPa and the ratio of $^{12}CH_3OH$ to ^{13}CO was 1:75. All experiments were carried out at CO conversions below 1 %. The most abundant reaction products were $^{13}CH_3OH$ and $^{13}CO_2$. Ethanol, 1-propanol, isobutanol, methyl formate, and methyl acetate were also detected and their formation rates as a function of residence time are shown in Figure 2.
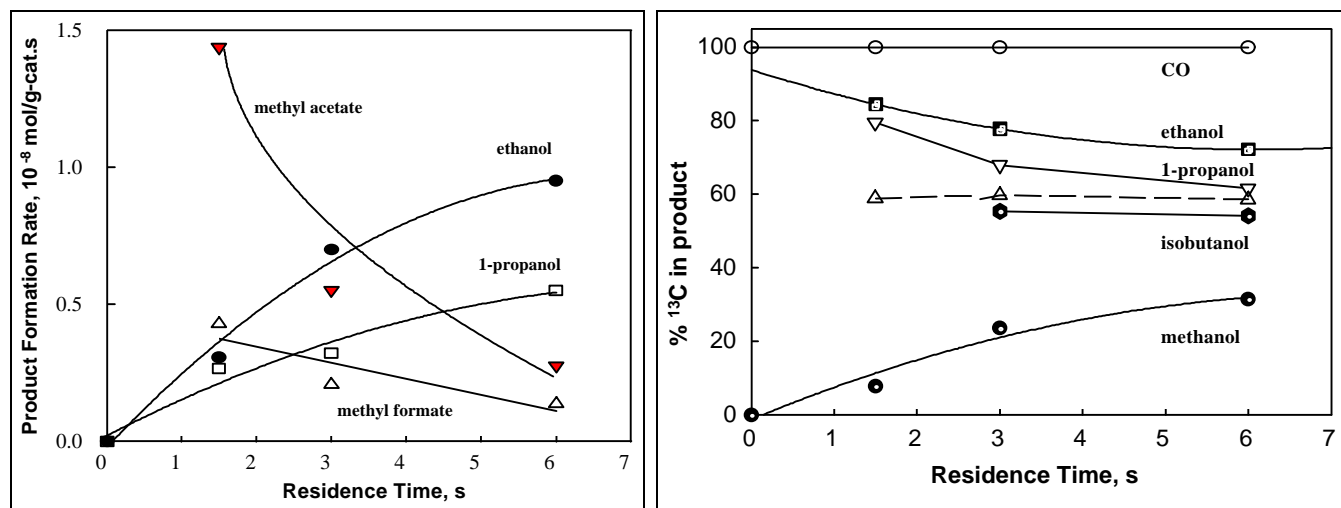
Figure 2. (a) Effect of bed residence time on product formation rate for 1.0 wt % $K-Cu_{0.5}Mg_5CeO_x$. (b) Effect of bed residence time on product carbon-13 distribution for 1.0 wt % $K-Cu_{0.5}Mg_5CeO_x$. [538 K, 2.0 MPa, $^{13}CO/H_2/CH_3OH = 100/100/1.3$]

The increased formation rates of ethanol and 1-propanol with increasing residence time suggest that they are secondary reaction products (Figure 2a). The formation rates of methyl formate and methyl acetate decrease with increasing residence time, suggesting that they are reaction intermediates or approach thermodynamic equilibrium. ^{13}C contents as a function of bed residence time are shown in Figure 2b for each alcohol product detected. The ^{13}C content in methanol increases with increasing bed residence time because ^{13}CO hydrogenation leads to the formation of labeled methanol. The ^{13}C content in ethanol decreases with increasing bed residence; extrapolation of the ethanol isotopic content to zero residence time shows that the initial ethanol product is predominantly labeled (94 % ^{13}C content). Thus, ethanol is formed predominantly by direct reactions of ^{13}CO without significant involvement of the $^{12}CH_3OH$ present in the feed.

At longer residence times, ethanol is also formed by reverse aldol reactions of higher alcohols, which contain lower ^{13}C contents because of the significant involvement of $^{12}CH_3OH$ in their formation. This reverse reaction leads to the observed decrease in ^{13}C content in ethanol with increasing residence time. The ^{13}C contents in 1-propanol calculated by assuming 1-propanol formed exclusively from methanol addition to ethanol via aldol-condensation reactions (dashed line in

figure 2b) is, however, lower than experimental values. This indicates that some 1-propanol is formed by carbonylation of C_2H_5OH by ^{13}CO. This is consistent with linear chain growth pathways that lead to the formation of some 1-butanol during CO hydrogenation on $K-Cu_{0.5}Mg_5CeO_x$.

Isotopic tracer studies using a mixture of $^{13}CO/H_2$ and $^{12}CH_3OH$, however, have shown that ethanol is predominantly unlabeled (14% ^{13}C content) at short bed residence time on $Cs-CuZnAlO_x$ (Figure 3), suggesting that it forms by the direct coupling reactions of methanol or its derivatives. The labeled ethanol at zero residence time may form directly from ^{13}CO following the pathways described for $K-Cu_{0.5}Mg_5CeO_x$. The predominant pathway for the formation of ethanol on Cs-promoted $CuZnAlO_x$, however, is the coupling of methanol as reported by others[4]. This is significantly different from the predominant pathway involving the direct reactions of CO on $Cu_{0.5}Mg_5CeO_x$.
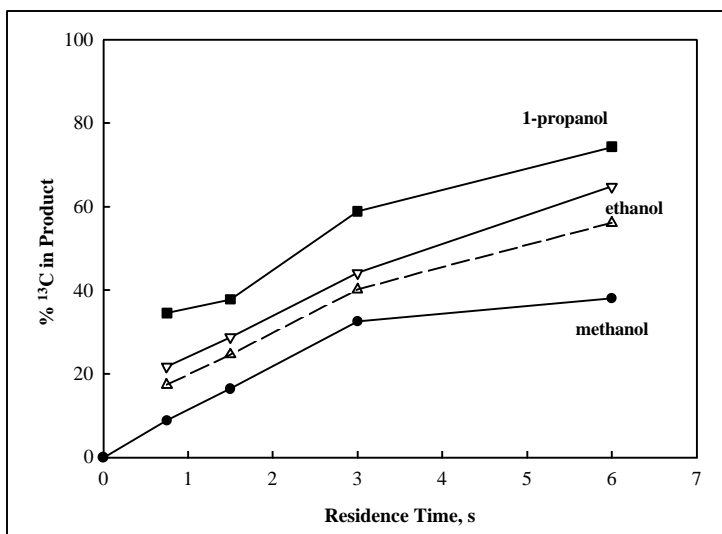
Figure 3. Effect of bed residence time on product carbon-13 distribution for $Cs-CuZnAlO_x$. [538 K, 2.0 MPa, $^{13}CO/H_2/^{12}CH_3OH = 100/100/1.3$]

Condensation Reactions of Alcohols

Ethanol dehydrogenation and coupling reactions were carried out in order to probe reaction pathways involved in branched and linear higher alcohols synthesis from methanol, ethanol, and propanol intermediates formed initially during CO hydrogenation reactions at high pressures. These studies also address the roles of Cu, K, and Mg-Ce oxides in the ethanol coupling reactions. The experiments were carried out on Mg_5CeO_x, 0.8 wt % $K-Mg_5CeO_x$, $Cu_{0.5}Mg_5CeO_x$, and 1.0 wt % $K-Cu_{0.5}Mg_5CeO_x$, and 1.2 wt % $K-Cu_{7.5}Mg_5CeO_x$ at atmospheric pressure.

Acetaldehyde was the predominant product of reactions of pure ethanol on 1.0 wt % $K-Cu_{0.5}Mg_5CeO_x$ (Figure 4a). Dehydrogenation reactions occur much faster than chain growth; the latter reaction leads to the formation of acetone, n-butyraldehyde, and other oxygenates (Figure 4a). Acetaldehyde reaches a maximum concentration at intermediate contact times during ethanol reactions and then decreases gradually. The acetaldehyde concentration at this point corresponds to the acetaldehyde concentration calculated from the thermodynamic equilibrium of the chemical reaction:

$$C_2H_5OH \; \rightleftharpoons \; C_2H_4O \; + \; H_2$$

The small decrease in acetaldehyde concentration at long contact times could be caused by further reaction of acetaldehyde to secondary products and/or a reversal of the ethanol-acetaldehyde equilibrium as ethanol is converted to chain growth products. Acetone and n-butyraldehyde were the predominant condensation products. The non-zero initial slopes on acetone and n-butyraldehyde curves (Figure 4a) are inconsistent with their formation only in sequential reactions of gas phase acetaldehyde intermediates:

$$C_2H_5OH \; \rightleftharpoons \; C_2H_4O \; \longrightarrow \; \text{Condensation products}$$

Therefore, condensation products are either formed directly by ethanol self-condensation or directly from acetaldehyde but at reaction rates independent of acetaldehyde concentration (Figure 4b). Methyl-ethyl ketone (by acetaldehyde self-condensation with intramolecular hydride shift before dehydration), 2-pentanone (by acetaldehyde-acetone

condensation), 2-propanol (by hydrogenation of acetone), 1-butanol (by hydrogenation of n-butyraldehyde), and ethyl acetate (by ethanol-acetaldehyde) were also detected in much smaller concentrations than n-butyraldehyde and acetone among reaction products.
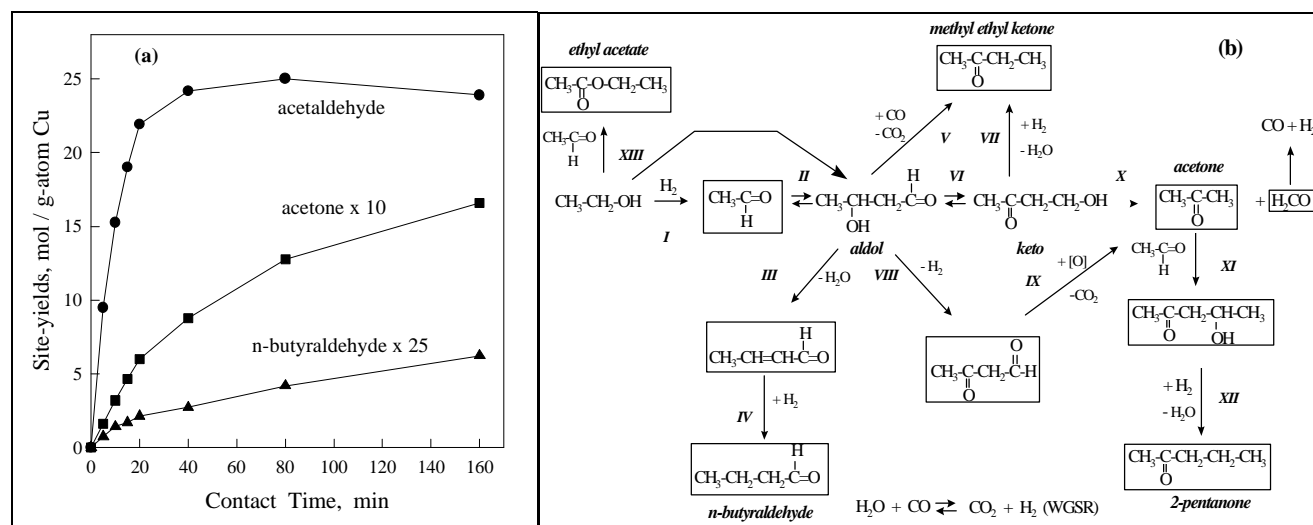
Figure 4. (a) Site yields as a function of contact time on 1.0 wt % K-Cu$_{0.5}$Mg$_5$CeO$_x$ in ethanol reactions. (b) Reaction scheme. [573 K, 101.3 kPa total pressure, 4.0 kPa ethanol, balance He]

Ethanol reaction rates and the selectivities to acetaldehyde, n-butyraldehyde, and acetone were measured on K-Cu-MgCeO$_x$ catalysts with a range of Cu and K contents in order to examine the role of Cu and basic sites on dehydrogenation and condensation reactions. The results are shown in Table 3. Initial dehydrogenation rates were very low on both Cu-free catalysts and ethanol conversion reached a limiting value of about 9 % after 0.33 h; this conversion value is much lower than the predicted equilibrium conversion (90 %) at these reaction conditions. Dehydrogenation rates were much higher on Cu-containing catalysts than on Mg$_5$CeO$_x$, suggesting that Cu sites catalyze ethanol dehydrogenation to acetaldehyde. The presence of K decreased areal ethanol dehydrogenation rates, because K decreases Cu dispersion. Ethanol dehydrogenation turnover rates on Cu$_{0.5}$Mg$_5$CeO$_x$, 1.0 wt % K-Cu$_{0.5}$Mg$_5$CeO$_x$, and 1.2 wt % K-Cu$_{7.5}$Mg$_5$CeO$_x$ catalysts were 0.24, 0.23 and 0.24 s^{-1}, respectively. Thus, ethanol dehydrogenation steps require exposed Cu atoms for the rate-determining step. Surface Cu atoms become unavailable for both N$_2$O decomposition and alcohol dehydrogenation when covered with K species and when Cu crystallites grow. Dehydrogenation turnover rates are not affected by Cu crystallite size or by the titration of a fraction of the Cu surfaces with KO$_x$ species.

Table 3. Effects of Cu- and K-loading on Ethanol Consumption and Product Formation on Mg$_5$CeO$_x$.

| Cu wt % | K wt % | Ethanol dehydrogenation | | Rates of formation | | | |
| | | areal rate $^a r_1$ | turnover rate $^b r_1$ | Acetone+2-Propanol | | Butyraldehyde+Butanol | |
				areal rate ($^c r_2$)	turnover rate ($^d r_2$)	areal rate($^c r_3$)	turnover rate ($^d r_3$)
0	0	4.0 x 10^{-9}	-	7.5 x 10^{-11}	7.9 x 10^{-5}	2.8 x 10^{-11}	2.9 x 10^{-5}
0	0.8	3.4 x 10^{-9}	-	9.7 x 10^{-11}	5.6 x 10^{-5}	1.6 x 10^{-10}	9.4 x 10^{-5}
7	0.1	3.6 x 10^{-7}	0.24	3.0 x 10^{-9}	2.2 x 10^{-3}	4.5 x 10^{-10}	3.4 x 10^{-4}
7	1.0	2.4 x 10^{-7}	0.23	4.3 x 10^{-9}	1.8 x 10^{-3}	7.6 x 10^{-10}	3.2 x 10^{-4}
49	1.2	9.4 x 10^{-7}	0.24	4.4 x 10^{-8}	1.0 x 10^{-2}	1.2 x 10^{-9}	2.8 x 10^{-4}

^{a} r_1 is the rate of ethanol consumption, in mol / m^2 total · s; ^{b} Turnover rates per Cu surface atom, in s^{-1}; ^{c} r_2 and r_3 are the rates of product formation, in mol / m^2 MgCeO$_x$ · s; ^{d} Turnover rates per accessible site from ^{13}CO$_2$/^{12}CO$_2$ in mol / mol basic site · s; basic sites measured by ^{13}CO$_2$/^{12}CO$_2$ isotopic switch method.

Aldol coupling chain growth rates are lower on Mg_5CeO_x than on $Cu_{0.5}Mg_5CeO_x$ because of lower acetaldehyde concentrations when Cu sites are not present. K increases the rate of base-catalyzed aldol coupling reactions to acetone and butyraldehyde (Table 3), even though steady-state acetaldehyde concentrations on $Cu_{0.5}Mg_5CeO_x$ and 1.0 wt % K-$Cu_{0.5}Mg_5CeO_x$ catalysts are similar. The total rates of base-catalyzed aldol coupling reactions, when normalized by the number of accessible basic sites, are similar on $Cu_{0.5}Mg_5CeO_x$ (2.5×10^{-3} s^{-1}) and K- $Cu_{0.5}Mg_5CeO_x$ (2.2×10^{-3} s^{-1}). Aldol condensation rates on 1.2 wt % K-$Cu_{7.5}Mg_5CeO_x$ (49 wt % Cu, 0.047 Cu dispersion) are, however, much higher than on catalysts with lower Cu content, even though the density of basic sites is similar on these two samples. The difference in condensation rates suggests that Cu sites are involved in rate-determining steps required for condensation reactions, even though such Cu sites are present in sufficient number to ensure ethanol-acetaldehyde thermodynamic equilibrium. The lower aldol coupling chain growth reaction rates observed on Cu-free catalysts, which are caused not only by the low concentration of required acetaldehyde intermediates but also by the absence of Cu sites required in condensation steps, are consistent with this proposal. More detailed reaction pathways about the role of Cu on the bifunctional mechanism for aldol-type condensation are reported elsewhere.[3,5] Additional experiments have shown that condensation, hydrogenation, and total conversion rates are approximately first order in acetaldehyde.[5] Reactions of $^{12}C_2H_5OH/^{13}C_2H_4O$ mixtures suggest that the condensation reaction can proceed via two parallel pathways: direct reactions of ethanol without the intermediate formation of gas phase acetaldehyde molecules and sequential dehydrogenation to form acetaldehyde followed by condensation steps.[5] These results show that the "dehydrogenation" and condensation steps occur on the same type of active site, an acid-base site pair on MgO. This proposal is consistent with the promoting effect of Cu on condensation rates, with the initial non-zero slopes of product formation observed in ethanol reactions, and with ^{13}C content in condensation products of $^{12}C_2H_5OH-^{13}C_2H_4O$ mixtures.

Ethanol is a useful and simple probe molecule to test the role of individual components in metal-base bifunctional catalysts for isobutanol synthesis. Ethanol reactions, however, lead to acetone and n-butyraldehyde, which form only 2-propanol and 1-butanol, after subsequent hydrogenation, during CO/H_2 reactions. 2-Propanol and 1-butanol cannot, however, form isobutanol precursors (such as isobutyraldehyde and propionaldehyde) by condensation reactions during CO hydrogenation. ^{13}C-tracer studies of methanol-acetaldehyde and methanol-propionaldehyde cross-coupling reactions were carried out in order to examine reaction pathways that lead to the formation of the C_3 and C_4 oxygenate precursors required for isobutanol formation via aldol-type reactions of alcohols and aldehydes with methanol-derived C_1 species. Reaction pathways involved in the formation of all detected products obtained on cross-coupling reactions for $^{13}CH_3OH-^{12}C_2H_4O$ mixtures on $Cu_{0.5}Mg_5CeO_x$ are shown in Figure 5a. The $^{13}CH_3OH$ component in the feed reacted predominantly to form ^{13}CO and H_2; this reaction reverses methanol synthesis because of unfavorable methanol synthesis thermodynamics at atmospheric pressures, but not during CO hydrogenation at high pressures. The ethanol reaction product was predominantly unlabeled and it forms by hydrogenation of acetaldehyde using Cu sites and hydrogen produced by methanol decomposition. Propionaldehyde contains predominantly one ^{13}C atom, suggesting that it is formed by condensation of acetaldehyde with reactive formyl or methoxy-type surface species or with gas phase formaldehyde derived from methanol. The labeled carbon was either in the CH_3 or the CHO fragment in propionaldehyde, suggesting that aldol condensation reactions occur with retention of either one of the two oxygen atoms in aldol-keto species as proposed by Nunan et al..[6,7] Both normal and oxygen retention reversal types of aldol condensation occurred on K-$Cu_yMg_5CeO_x$ catalysts. These types of reactions are caused by interconversion of aldol and keto species via rapid intramolecular H-transfer (Figure 5b). Isobutyraldehyde contained predominantly two ^{13}C atoms, suggesting that it forms by condensation of propionaldehyde (with one ^{13}C) with a C_1 species formed from methanol. Acetone and n-butyraldehyde showed no significant ^{13}C-enrichment and they formed only by self-condensation reactions of acetaldehyde or ethanol. Only traces of labeled ethanol were detected among reaction products, suggesting that methanol coupling reactions, previously proposed as a route for C_1 to C_2 chain growth during higher alcohol synthesis,[4] do not readily occur at the low pressures. In contrast with high pressure CO hydrogenation conditions, our reaction conditions favor the decomposition of methanol and minimize its bimolecular chain-growth reactions.
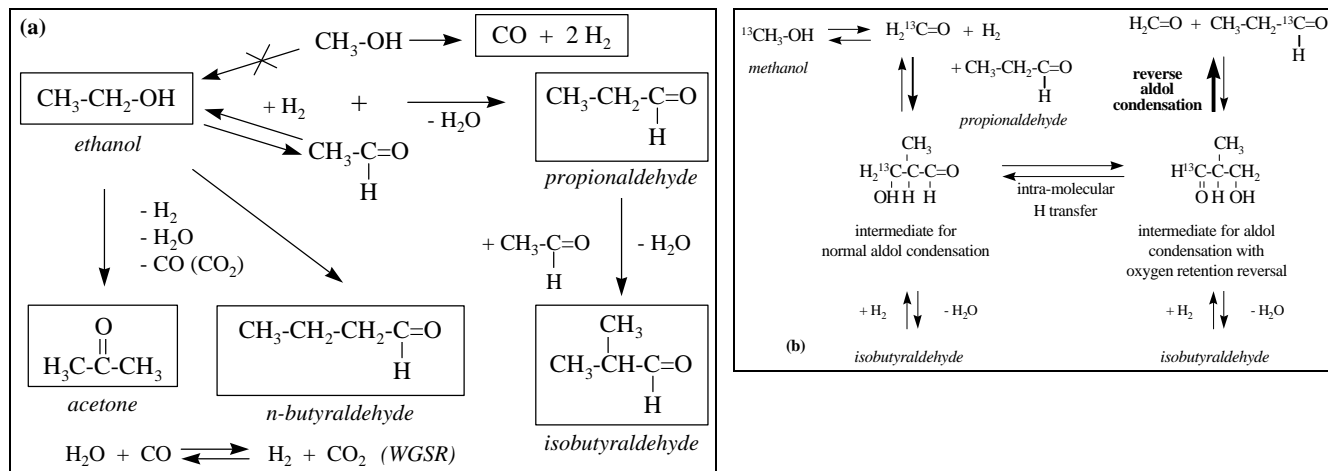
Figure 5. (a) Reaction scheme for methanol-acetaldehyde reactions. (b) Reaction scheme of the labeled propionaldehyde production.

Reactions of propionaldehyde-^{13}C-methanol mixtures confirm these condensation pathways. These studies also show that aldol formation and dehydration-decarbonylation pathways are reversible. CO_x and H_2 (from methanol decomposition and water-gas shift reactions), isobutyraldehyde, 1-propanol, and methyl propionate were the main reaction products. Other products included methyl formate, 3-pentanone (from propionaldehyde self-condensation followed by decarboxylation), and 2-methyl-pentaldehyde (from propionaldehyde self-condensation). 2,2-dimethyl butyraldehyde (from cross coupling of isobutyraldehyde and C_1 species) was not observed, indicating that isobutyraldehyde is a preferred end-product of chain growth reactions. Neither ethanol nor acetaldehyde were detected. The results obtained from quantitative analysis of the isotopic content for propionaldehyde-^{13}C-methanol coupling reactions on 1.0 wt % K-Cu$_{0.5}$Mg$_5$CeO$_x$ show that propionaldehyde acquires some ^{13}C during reaction. The increment in the ^{13}C content in propionaldehyde molecules as a function of contact time can be explained by the scheme showed in Figure 6b. The proposed pathway includes the formation of surface aldol species (from propionaldehyde and C_1 intermediates), keto-enol transformation (by intramolecular H-transfer), and reverse aldol condensation from the keto form leading to propionaldehyde and C_1 species. Isobutyraldehyde is predominantly labeled with one ^{13}C, suggesting that it forms most frequently by cross coupling reactions between ^{13}C-labeled methanol and propionaldehyde. Isobutyraldehyde with two ^{13}C forms by aldol condensation reactions of labeled methanol with singly-labeled propionaldehyde formed by retro-aldol reactions.

Acknowledgments

References

1. J.G. Nunan, R.G. Herman, and K. Klier, *J. Catal.* **116**, 222 (1989).
2. C.R. Apesteguia, S.L. Soled, S. Miseo, *US Patent* 5,387,570.
3. M. Xu, M. J.L. Gines, B.L. Stephens, A.-M. Hilmen, and E. Iglesia, *J. Catal.*, in press.
4. J.G. Nunan, C.E. Bogdan, K. Klier, K.J. Smith, C.-W. Young, and R.G. Herman, *J. Catal.* **113**, 410 (1988).
5. M.J.L. Gines, and E. Iglesia, submitted to *J. of Catal.*.
6. J.G. Nunan, C.E. Bodgan, K. Klier, K.J. Smith, C. Young, and R.G. Herman, *J. Catal.* **116**, 195 (1989).
7. J.G. Nunan, C.E. Bodgan, R.G. Herman, and K. Klier, *Catal. Lett.* **2**, (1989) 49.